Penetration Model for Installation of Skirted Foundations in Layered Soils

Rasmus Tofte Klinkvort[1]; Hendrik Sturm[2]; and Knut H. Andersen, M.ASCE[3]

Abstract: During installation of a skirted foundation, resistance to penetration is a combination of side and tip resistances. When penetrating a permeable soil unit, tip resistance in particular can be high but if seepage water flow from the outside to the inside of the skirted foundation exists, the pore water gradient will reduce the effective stresses and therefore also penetration resistance. Recent installation data from the field and laboratory suggest that this effect can also occur during installation in layered profiles. This paper presents a model that accounts for seepage flow in unlimited permeable layers that are overlain by one or several impermeable layers. The model assumes that seepage flow in the underlying sand layer is induced by an incremental lift of the internal soil plug, which enables the transfer of some of the differential pressure applied under the foundation lid to the bottom of the lifted soil plug. A single equation is proposed to calculate the critical suction number for layered soil conditions that can be used with an empirical model to calculate the reduction in penetration resistance. A calibration of the proposed equation for the critical suction number is carried out using an axis symmetrical finite-element model that uses a linear elastic soil model and assumes steady-state flow conditions. The calibration of the proposed equation for calculating the critical suction number was first carried out for a homogenous permeable soil. This was done to benchmark the model against previously published data. In a second step, the calibration was done for a layered profile and different flow boundary conditions. The proposed penetration model is demonstrated by back-calculating full-scale installations. The paper closes with a discussion of the main assumption of plug lift, and a simple model to evaluate the degree of plug lift is proposed. **DOI: 10.1061/(ASCE)GT.1943-5606.0002106.**

Author keywords: Suction caisson; Skirted foundations; Installation; Layered soils; Offshore wind.

Introduction

Skirted foundations or suction caissons have been used for several years in oil and gas projects for both clay profiles (Andersen et al. 2005) and sand profiles (Tjelta 1994). Skirted foundations are also now considered on a routine basis as foundations for offshore wind turbines. The soil conditions at many wind farms currently under development often comprise layered profiles consisting of clay, silt, and sand. The installation stage for foundations poses a particular risk that needs to be considered when evaluating potential foundation concepts, and therefore a reliable installation model is an essential tool for this evaluation (Sturm 2017).

The total penetration resistance, Q_{tot}, is the sum of friction on the skirt wall(s), Q_{side}, and the resistance of the skirt tip, Q_{tip}. The side friction is computed along the vertical surfaces inside and outside the skirt wall(s), whereas tip resistance is calculated using the horizontally projected tip area of the skirt. This is shown in Eq. (1)

$$Q_{tot} = Q_{side} + Q_{tip} = \sum \tau_{side} \times A_{side} + q_{tip} \times A_{tip} \qquad (1)$$

In general, the installation of a skirted foundation comprises two phases: a self-weight penetration phase, where the skirt penetrates into the soil by its self-weight; and a suction phase, where a pump is used to lower the pressure inside the foundation, creating a differential pressure that will force the foundation into the ground. Several methodologies to estimate penetration resistance for both phases of the installation have been proposed (Houlsby and Byrne 2005a, b; Andersen et al. 2008; Senders and Randolph 2009). When a suction caisson penetrates low-permeability layers (e.g., clay), the soil exhibits undrained behavior; undrained strength is often used to compute resistance. When a suction caisson penetrates a high-permeability layer (e.g., sand), drained strength and the associated angle of friction are often used together in an effective stress analysis to compute resistance. If the differential pressure generates a seepage flow in the soil from the outside to the inside of the foundation caisson, the effective stresses around the skirt tip and along the inside skirt wall are reduced, thereby also reducing penetration resistance. This mechanism is well understood and has been documented in several publications (Erbrich and Tjelta 1999; Houlsby and Byrne 2005a; Tran et al. 2005; Tran and Randolph 2008; Andersen et al. 2008; Senders and Randolph 2009). The lowest penetration resistance in high permeability layers is achieved when the upward flow gradient in the soil plug is equal to the vertical effective stresses at rest. This corresponding gradient is denoted the critical gradient. Because tip resistance in sand contributes most to total penetration resistance when omitting the effect of seepage flow in the soil, a significant reduction in tip resistance is obtained when a critical gradient is achieved because it triggers a local bearing failure of the soil below the tip and toward the inside of the caisson. Thus, the largest benefit of a suction-supported installation in sand is achieved when the applied pressure difference approaches the critical gradient in the soil.

[1]Senior Consultant, Norwegian Geotechnical Institute, Sognsveien 72, Oslo 0855, Norway (corresponding author). Email: rtk@ngi.no

[2]Technical Lead Offshore Renewables, Norwegian Geotechnical Institute, Sognsveien 72, Oslo 0855, Norway. ORCID: https://orcid.org/0000-0002-2340-8936. Email: hendrik.sturm@ngi.no

[3]Technical Expert, Norwegian Geotechnical Institute, Sognsveien 72, Oslo 0855, Norway. Email: knut.h.andersen@ngi.no

Note. This manuscript was submitted on May 13, 2018; approved on March 11, 2019; published online on August 2, 2019. Discussion period open until January 2, 2020; separate discussions must be submitted for individual papers. This paper is part of the ***Journal of Geotechnical and Geoenvironmental Engineering***, © ASCE, ISSN 1090-0241.

Erbrich and Tjelta (1999) introduced a suction number (S_N), which is the normalization of the applied differential pressure by the initial vertical effective stress at the skirt tip (σ'_v). The critical suction number, $S_{N,cr}$, is the applied differential pressure (suction) that generates a critical gradient. The normalization is shown in Eq. (2), where Δu is the differential pressure, H is the differential water head, z is the current penetration depth into the permeable layer, γ' is the effective unit weight of the permeable layer, and γ_w is the unit weight of water

$$S_N = \frac{\Delta u}{\sigma'_v} = \frac{\Delta u}{z \times \gamma'} = \frac{H}{z} \times \frac{\gamma_w}{\gamma'} \tag{2}$$

The gradient is not constant within the soil plug and varies in both radial and axial directions, which was also shown in Erbrich and Tjelta (1999). It is, though, widely accepted to use the exit gradient at a point inside the caisson (also shown on Fig. 3) that is immediately adjacent to the skirt at the soil surface as a reference value for the entire plug (Erbrich and Tjelta 1999; Andersen et al. 2008).

It is often assumed that no flow of water is generated in a sand layer that is overlain by clay. Houlsby and Byrne (2005b) and Tran (2005) provide discussions on this point. The potential for a large plug lift and for high tip resistance in the sand layer is the main reason to either avoid these locations, only penetrate into the clay, or modify anchors with flow channels to ensure the flow of water through the sand layers, as detailed in Aas et al. (2009). However, several recent installations indicate that a seepage flow can be mobilized in a sand layer that is overlain by an impermeable layer (Houlsby and Byrne 2005b; Saue et al. 2017; Panayides et al. 2017). This has also been observed in centrifuge tests reported by Watson et al. (2006), Tran et al. (2007), and Senders et al. (2007). Senders et al. (2007) proposed a simple model to predict penetration into a layered profile of clay overlain by sand, but the model does not account for the effect of the clay under the sand layer, nor does it include a model to estimate soil plug lift. In this paper, we define plug lift as the layer or layers above the permeable flow layer that lift upward without changing volume.

This paper presents an extended calculation procedure for penetration in sand based on the method proposed by Andersen et al. (2008). It extends already established relationships so that they also account for the effect of an impermeable layer underneath the caisson and the effect of an impermeable layer above the suction caisson tip. The extension is based on a revised engineering model and a numerical parametric study on seepage water flow, which includes the effect of impermeable top layers and also the effect of an approaching impermeable layer. These finite-element analyses reflect the boundary conditions of the revised engineering model, and the results are used to calibrate a mathematical formulation to calculate the critical suction number. The critical suction number is then used to calculate a reduction in penetration resistance similar to the approach given in Andersen et al. (2008). The performance of the extended model is demonstrated on some recent suction anchor installations into layered soil profiles. A discussion of the plug lift is given, and a model to predict the plug lift is proposed.

Extended Flow Model

The model is based on the procedure presented in Andersen et al. (2008), but is extended to cover additional flow situations. The model considers three different boundary conditions: a condition with no flow, denoted No Flow, where the soil is so impermeable that no significant seepage occurs in the soil; a flow condition denoted Pure Flow, where water flows through the entire soil plug from the outside surface to the inside surface; and a flow condition denoted Part Flow, where there is local seepage around the skirt tip. The two flow conditions can, in addition, take into account the effect of the underlying impermeable layer, which is gradually approached by the penetrating skirt tip. The calculation of the No Flow condition can be done by already existing methods, and this paper describes only the Pure Flow and Part Flow conditions. In short, the approach follows the same steps as in Andersen et al. (2008) and calculates the following:

- Penetration resistance assuming No flow, similar to Andersen et al. (2008). This can be found using, for example, an empirical cone penetration testing (CPT) model, where $Q_{tip} = k_{tip} \times q_c \times A_{tip}$ and $Q_{side} = A_{wall} \times \int k_{side} q_c(z) dz$.
- Critical suction number ($S_{N,cr}$) depending on flow condition (Part Flow or Pure Flow), an extension of the Andersen et al. (2008) model.
- Penetration resistance taking flow condition into account, similar to Andersen et al. (2008).

Fig. 1 shows a sketch of the model with the definition of the different parameters of a skirted foundation during suction-supported installation in a layered soil profile. Here z_{pen} is used as the total penetration depth of the skirt, z as the penetration depth into the permeable layer, and z_t as depth of layer/layers with no water seepage flow. The Hvorslev equation is valid for a case with only a permeable layer, a situation described in Andersen et al. (2008). It is here noted that, even though model calibration is carried out with only one low permeable layer, the model is also valid for a situation with several low impermeable layers. In this case, depth, z_t, shown on Fig. 1, will be from the top seafloor down to the lowest low permeable layer. The calculation of No Flow resistance can be carried out using CPT-based models (e.g., Senders et al. 2007; Andersen et al. 2008) or in using bearing capacity approaches e.g., Houlsby and Byrne 2005a, b; Andersen et al. 2008). The main idea of the extended model is that the pressure difference applied to the soil plug is partially transferred to the top of an underlying permeable sand layer by means of a lift of the impermeable layer (plug lift). Water starts to flow as a result of the pressure difference that now exists between the top of the permeable layer inside the skirt and the soil outside the skirt. This is similar to the assumption in Senders et al. (2007). This seepage reduces effective stresses and corresponding penetration resistance.

To calculate the critical suction ($S_{N,cr}$), a modification of Hvorslev's (1951) analytical solutions for flow (q) in a well with

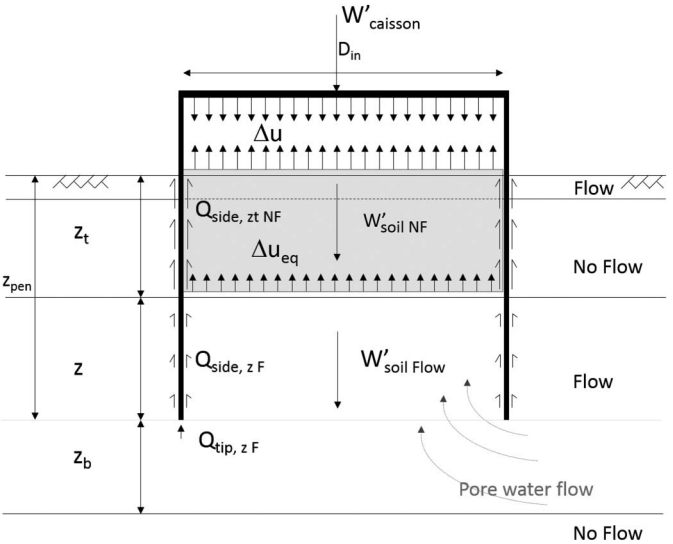

Fig. 1. Sketch of suction caisson installation model specifications.

casing in uniform soil is proposed. The modification is shown in Eq. (3) in a normalized form as

$$\frac{q}{k_i} = \frac{H}{z} \times \frac{\frac{11z}{4D} + \delta}{\alpha \times \left(\frac{\pi k_i}{4k_o} + \beta + \frac{11z}{4D} \times \chi\right)} \tag{3}$$

The fitting parameters α, χ, β, and δ are not in the original Hvorslev (1951) solution, but when $\alpha = \chi = 1$ and $\beta = \delta = 0$, Eq. (3) is identical to the Hvorslev solution. The fitting parameters are here introduced to take the distance to an impermeable layer and the flow evaluation point into account. Hvorslev (1951) calculates the average flow, whereas the modification allows flow at a given point to be calculated. With flow calculated from permeability and gradient ($i/q = k$), Eqs. (2) and (3) can be rewritten to evaluate the critical suction number as presented in Eq. (4). The formulations given in Eqs. (3) and (4) are general and are valid for both Pure Flow and the Part Flow conditions. The four additional parameters that are introduced are calibrated by a parametric study presented later

$$S_{N,\mathrm{cr}} = \alpha \times \frac{\gamma_w}{\gamma'} \times \frac{\frac{\pi}{4}\frac{k_i}{k_o} + \beta + \frac{11}{4}\frac{z}{D} \times \chi}{\frac{11}{4}\frac{z}{D} + \delta} \tag{4}$$

where k_i/k_o = ratio between permeability inside and outside the skirt; z/D = normalized skirt penetration into the flow layer; z_b/D = normalized distance from skirt tip to the deeper impermeable layer; and γ_w/γ' = ratio of unit weight of water and effective unit weight of soil in the flow layer.

For a Pure Flow condition ($z_t = 0$)

$$\alpha = \frac{4.8623}{16.1833\frac{z_b}{D}} + 0.9701, \qquad \beta = 1.9338 - \tanh\left(\frac{\frac{z_b}{D} + 0.1273}{0.2282}\right),$$

$$\chi = -0.4163 + \tanh\left(\frac{\frac{z_b}{D} + 0.0498}{0.4026}\right), \qquad \delta = \frac{0.8350}{4.6850\frac{z_b}{D}} + 0.5159$$

For a Part Flow condition ($z_t \geq 0$),

$$\alpha = 1.8981 - \tanh\left(\frac{\frac{z_b}{D} - 0.1377}{0.3883}\right), \qquad \beta = 0.45285,$$

$$\chi = 0.2315 + \tanh\left(\frac{\frac{z_b}{D} - 0.0306}{0.8673}\right),$$

$$\delta = -0.9150 + \tanh\left(\frac{\frac{z_b}{D} + 0.6402}{0.3472}\right)$$

Having found the critical suction number, the reduction in penetration resistance is found using the approach proposed by Andersen et al. (2008). In Andersen et al. (2008), several model and prototype installations were evaluated and it was found that the reduction in penetration resistance can be determined using the ratio of skirt thickness to penetration depth (z/t) and the critical suction number ($S_{N,\mathrm{cr}}$). The diagram for reduced penetration resistance as a function of suction number and aspect ratio, presented originally in Andersen et al. (2008), is replotted in Fig. 2 with a slight update to the proposed curves in order to describe the curves using closed-form mathematical equations. This update allows a better implementation of the model in numerical algorithms. It is noted that the original basis for the diagram is purely empirical and is only valid for Pure Flow sand profiles, but here it is used as an approximation also for Part Flow conditions. The term *Flow* is used here to refer to the common condition that includes both Pure Flow and the Part Flow.

The curves in Fig. 2 are described using the equation for a super ellipse

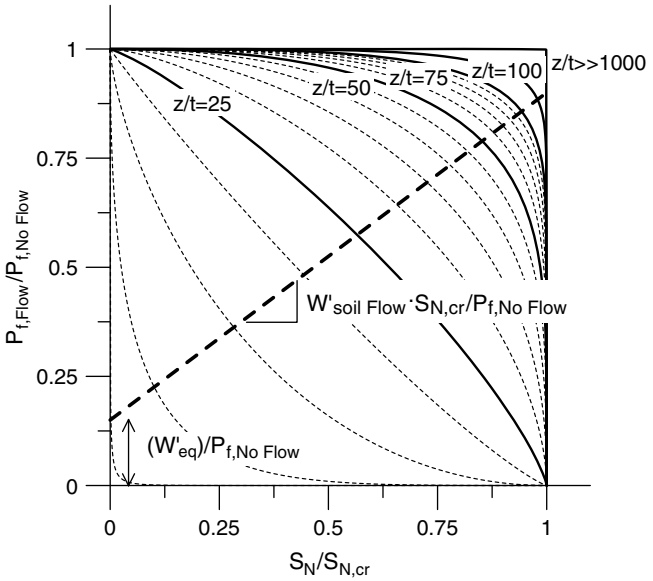

Fig. 2. Recommended diagram for reduced penetration resistance as a function of suction number and aspect ratio. (Adapted from Andersen et al. 2008.)

$$\frac{P_{f,\mathrm{Flow}}}{P_{f,\mathrm{NoFlow}}} = \left(1 - \left(\frac{S_N}{S_{N,\mathrm{cr}}}\right)^{0.05(z/t)}\right)^{\left(\frac{1}{0.0017(z/t)^2+0.2}\right)} \tag{5}$$

The driving force given is defined as a straight line

$$\frac{P_{f,\mathrm{Flow}}}{P_{f,\mathrm{No\ Flow}}} = \left(\frac{W'_{\mathrm{soil\ plug}} \times S_{N,\mathrm{cr}}}{P_{f,\mathrm{No\ Flow}}}\right)\left(\frac{S_N}{S_{N,\mathrm{cr}}}\right) + \frac{W'_{\mathrm{eq}}}{P_{f,\mathrm{No\ Flow}}} \tag{6}$$

The equivalent foundation weight for the Pure Flow condition is found as $W'_{\mathrm{eq}} = W'$ and for the Part Flow condition as $W'_{\mathrm{eq}} = W' + W'_{\mathrm{soil,eq}} - \mathrm{Q}_{\mathrm{outside},zt,\mathrm{NoFlow}}$ with W'_{eq} values limited to values ≥ 0.

Reduced penetration resistance ($P_{f,\mathrm{Flow}}/P_{f,\mathrm{No\ Flow}}$) in the permeable layer for the Part Flow or Pure Flow condition is found for values where Eq. (5) equals Eq. (6).

Calculation Procedure

With Eqs. (4)–(6), it is possible to calculate penetration resistance using a stepwise procedure that is similar to the one proposed by Andersen et al. (2008) but also takes into account the Pure Flow and Part Flow cases:

1. Calculate penetration resistance with no seepage flow (using CPT- or BC-based models) for all layers

$$Q_{\mathrm{side,No\ Flow}} \text{ and } Q_{\mathrm{tip,No\ Flow}}$$

2. Determine No Flow resistance in the permeable layer

$$Pf_{z,\mathrm{No\ Flow}} = Q_{\mathrm{side},z,\mathrm{No\ Flow}} + Q_{\mathrm{tip},z,\mathrm{No\ Flow}}$$

3. For the given Flow condition in the permeable layer, determine the critical suction number, $S_{N\mathrm{cr}}$, using Eq. (4) based on a Pure Flow or Part Flow condition, an estimated $k_{\mathrm{in}}/k_{\mathrm{out}}$ ratio based on Andersen et al. (2008), normalized skirt penetration depth into the permeable layer, z/D, and distance to the impermeable layer, z_b/D.

4. Calculate the equivalent foundation weight

$$W'_{\text{eq}} = \begin{cases} W' & \text{(for Pure Flow)} \\ W' + W'_{\text{soil eq}} - Q_{\text{outside},zt,\text{No Flow}} \geq 0 & \text{(for Part Flow)} \end{cases}$$

where

$$\text{W}'_{\text{soil eq}} = \pi/4 Din^2 z_t \gamma'$$

5. Calculate ratio between submerged equivalent foundation weight and No Flow penetration resistance

$$W'_{\text{eq}}/P_{f,z,\text{No Flow}}$$

and ratio in the permeable layer

$$W'_{\text{soil Flow}} S_{N\text{cr}}/P_{f,z,\text{No Flow}}$$

where

$$W'_{\text{soilFlow}} = \pi/4 D_{\text{in}}^2 z\gamma'$$

6. Determine penetration reduction in the permeable layer using Eqs. (5) and (6)

$$P_f/P_{f,\text{No Flow}} \text{ and } S_N/S_{N\text{cr}}$$

7. Determine total resistance for permeable layer

$$\text{P}_{\text{tot,Flow}} = \text{P}_{\text{tot},z,\text{No Flow}} \times (\text{P}_f/\text{P}_{f,z,\text{No Flow}})$$

8. Calculate total resistance for the given penetration depth (z_{pen}) as

$$P_{\text{tot}} = \begin{cases} P_{\text{tot,Flow}} & \text{(for Pure Flow)} \\ P_{\text{tot,Flow}} + Q_{\text{outside},zt,\text{No Flow}} + Q_{\text{inside},zt,\text{No Flow}} & \text{(for Part Flow)} \end{cases}$$

9. Find the required equivalent differential pressure at the top of the permeable layer

$$\Delta u_{\text{eq}} = 0 \text{(for Pure Flow)}$$
$$\Delta u_{\text{eq}} = (P_{\text{tot,Flow}-W'_{\text{eq}}})/A_{\text{in}} \text{(for Part Flow)}$$

10. Calculate the total required differential pressure as

$$\Delta u = \Delta u_{\text{eq}} + (W'_{\text{soileq}} + Q_{\text{inside},zt,\text{No Flow}})/A_{\text{in}}$$
$$\Delta u = (P_{\text{tot}} - W')/A_{\text{in}}$$

Calibration of the Extended Flow Model

The extended Flow model just presented is based on a series of finite-element (FE) analyses performed in the commercially available FE program. The engineering model of these analyses consisted of a circular sealed foundation (suction caisson with a diameter of 8 m) penetrated into a permeable soil layer. The permeable layer was assumed to be infinite in the horizontal direction and had different heights in the vertical direction. The FE discretization is shown in Fig. 3. Because the FE model was used only to evaluate seepage flow, the height of the impermeable layer was omitted in these analyses. The calculations were done in an axissymmetrical model with a horizontal radius of 40 m (5D) and a

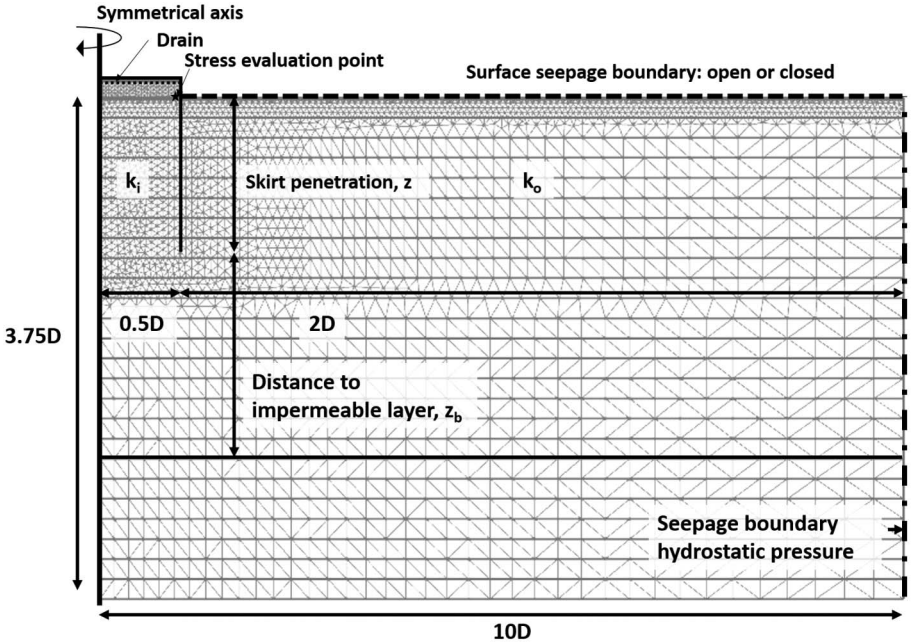

Fig. 3. Sketch of finite-element model and dimensions.

J. Geotech. Geoenviron. Eng., 2019, 145(10): 04019085

total depth of 30 m (3.75D). The analyses were carried out using a boundary line with a defined water head (drain) inside the caisson. The water head in this drain was, in all analyses, 1 m under the water head outside the caisson. Having a water head difference between inside and outside generates a flow from the outside to the inside. The gradient in the soil was evaluated at a stress integration point located close to the caisson skirt in the surface (Fig. 3). The other boundary conditions were as follows. The bottom of the domain was fixed in the horizontal and vertical directions, whereas the symmetry axis and the "infinite" vertical boundary at the right side in Fig. 3 were fixed in the horizontal direction. The surface boundary was free to move in all directions. At the outside boundaries of the model, a hydrostatic pore pressure distribution relative to the outside water head was applied. This was also applied to the free surface outside the caisson in the Pure Flow analyses. In the Part Flow analyses, no flow was allowed at the free surface at the outside of the caisson.

A parametric study was carried out using the following:

- Five inside to outside permeability ratios, $k_i/k_o = \{1, 2, 3, 4, 5\}$,
- Nine skirt penetration depths $z/D = \{0.0125, 0.125, 0.25, 0.375, 0.5, 0.625, 0.75, 0.875, 1\}$,
- Six distances to a lower impermeable layer $z_b/D = \{0.125, 0.25, 0.375, 0.5, 1, 2\}$, and
- Permeable and impermeable boundary conditions at the outside surface.

Each parameter was combined, leading to a total of 540 analyses. Care should be taken when using the proposed model outside its calibration range.

The flow analyses were carried out in an axis-symmetrical finite-element model discretized with 5,023 fully coupled stress equilibrium pore pressure 15-node triangular elements. The soil behavior was modeled using a linear elastic soil model and assuming steady state flow conditions.

Even though the model was calibrated only for z/D ratios between 0.0125 and 1, the equation that we propose follows the trend seen for larger ratios. The equations can therefore also be used for larger ratios within a reasonable accuracy.

Critical Suction Number

The flow (q) was evaluated at the stress integration point; based on this flow and the applied pressure difference (H), the critical gradient was calculated as shown in Eq. (7)

$$S_{N,\mathrm{cr}} = \frac{H \times k_i}{q \times z} \tag{7}$$

Fig. 4 shows the results of the Pure Flow analyses where the surface boundary is open, together with the new equation presented in Eq. (4). A comparison with the results from Erbrich and Tjelta (1999) and Andersen et al. (2008) is included in Fig. 4(a) for the case where there is a large distance to a lower impermeable layer. The results of the three analyses are practically identical. The small difference seen between the studies may be related to variation in the exact location where the gradient was evaluated. Nevertheless, the good comparison with previously presented studies confirms the validity of the FE model. The analyses show that the seepage flow and thereby the critical suction gradient was affected only by the impermeable layer when the distance between the skirt penetration depth and the impermeable layer was smaller than approximately $D/2$ (i.e., $z_b/D \leq 0.5$).

Similar analyses were carried out with an impermeable surface boundary. This boundary condition represented the Part Flow

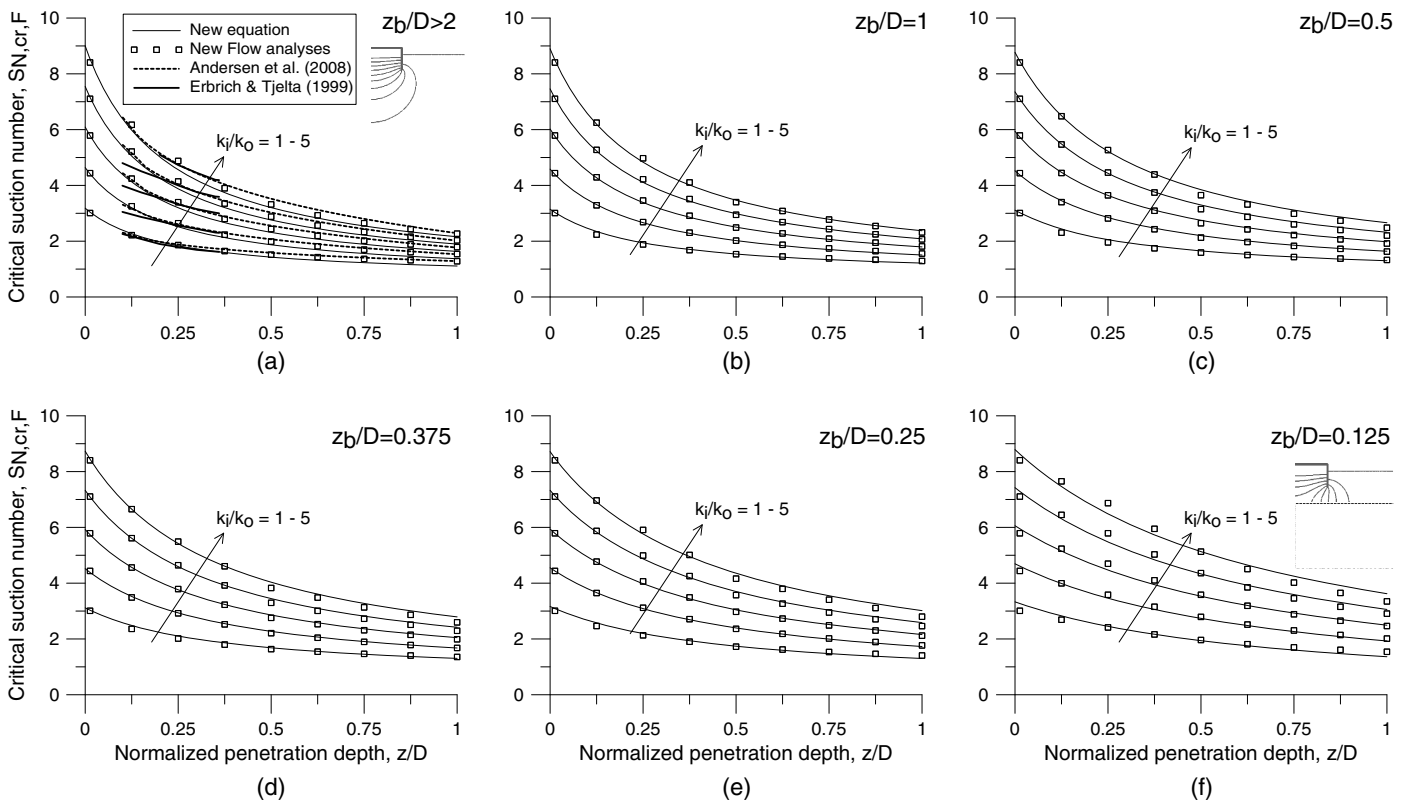

Fig. 4. Flow case–critical suction number as a function of normalized penetration, permeability ratio, and distance to normalized impermeable layer.

J. Geotech. Geoenviron. Eng., 2019, 145(10): 04019085

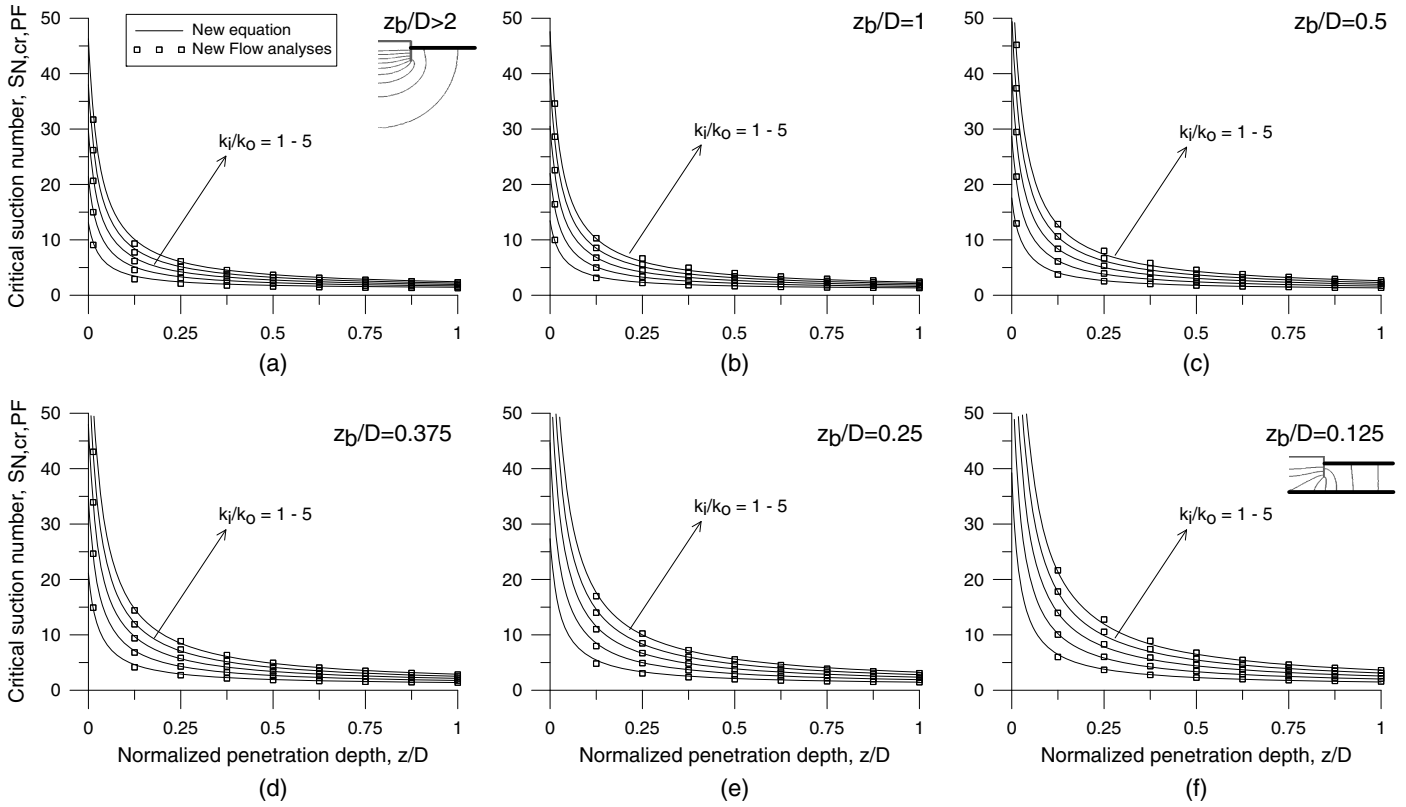

Fig. 5. Part Flow case–critical suction number as a function of normalized penetration, permeability ratio, and distance to normalized impermeable layer.

case where the skirt penetrated through an impermeable layer into a permeable layer. Fig. 5 presents the results of these analyses. The critical suction number is higher here compared to the Pure Flow situation, especially for short penetration depths. It is noted that, even though the critical suction numbers for short penetration depths and short distances to the impermeable layer are not included in all the graphs in Fig. 5; these points were used to calibrate the model. They were omitted from the figures because their values were so relatively large that they could not be shown within the present scale.

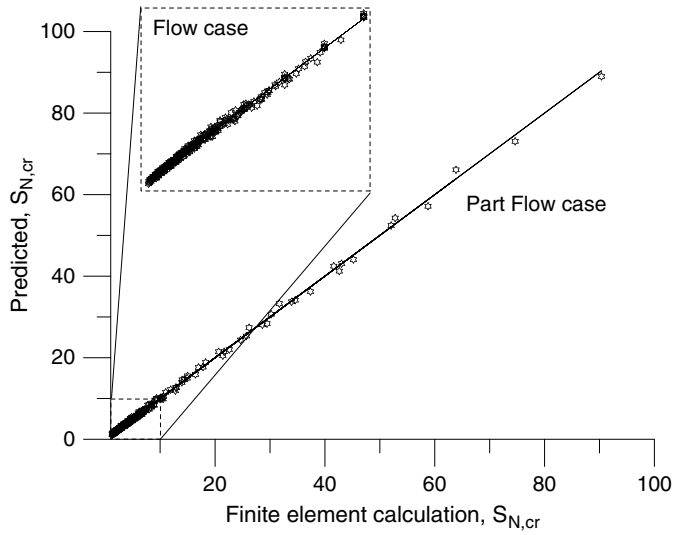

Fig. 6. Comparison of calibrated model and theoretical model.

To illustrate the accuracy of the calibrated flow models, the predicted results are compared with the results from the finite-element analyses in Fig. 6. It can be seen that the simple model calculates the critical suction number with a high degree of accuracy for all investigated analyses, including the very high values omitted from Fig. 5.

Average Flow in Part Flow Analysis

The water flow out of the caisson can be used to estimate the plug lift. The flow rate, q, was found using the proposed modification to Hvorslev's theoretical solution shown in Eq. (3). During the Part Flow analysis, the average flow over the caisson area was also evaluated. These flow rates were calculated using Eq. (3). The calibration was similar to previous calibrations except it was ensured that the factors used would predict correct or larger flow rates because this would provide an estimate of the plug lift on the safe side. From this calibration, the following factors, to be used with Eq. (3), were found. These factors are shown in Eq. (8)

$$\alpha = 1.9977 - \tanh\left(\frac{\frac{z_b}{D} - 0.3505}{0.7270}\right),$$
$$\beta = -0.7928 + \tanh\left(\frac{\frac{z_b}{D} + 0.9277}{0.9068}\right), \qquad \chi = 1,$$
$$\delta = -1.000 + \tanh\left(\frac{\frac{z_b}{D} + 6.4375}{0.6643}\right) \tag{8}$$

The predicted flow results are compared to the results from the finite-element analysis in Fig. 7 to show the quality of the calibration. The model does not show the same good match as seen with the critical suction number prediction, and it appears that the model

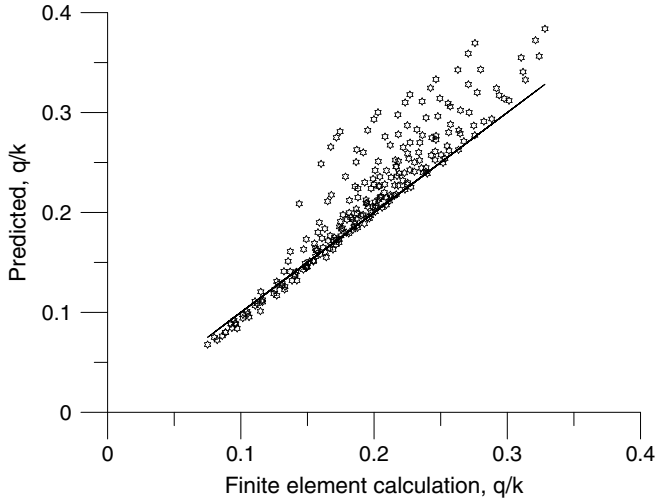

Fig. 7. Comparison of calibrated and theoretical models for average flow.

consistently overestimates the flow. As a result, this model will overestimate the soil plug lift, which is also regarded as acceptable.

Discussion

An extended flow model for penetration in layered soil profiles and a calibration of the necessary parameters needed for this model have been presented. This section discusses some of the assumptions used in the development of the model.

Elastic Soil Model

All flow analyses were performed using a linear elastic soil model, which does not capture the stress dependency of the soil stiffness and thereby affects the flow and introduces a small error. The fact that the model uses a combination of theoretical and empirical data masks this potential effect. An elastic soil model was also used in the previously proposed model (Andersen et al. 2008), together with the reduction in resistance shown in Fig. 2. The empirical observations are therefore linked to the calculation procedure, meaning that this effect is consider to be insignificant.

Penetration Resistance Reduction Model

The model used to assess reduced penetration resistance due to seepage (Fig. 2) is based on model tests and field observations of suction caisson penetration in permeable soil profiles (Pure Flow). This model is also used here to predict the reduction in penetration resistance due to seepage in permeable layers underlying an impermeable layer (Part Flow). The reduction model presented in Fig. 2 is therefore used outside its calibration range. In order to evaluate the validity of this assumption, different flow conditions were examined. Fig. 8 presents normalized water head potential lines for eight boundary conditions. These eight analyses represent the extreme boundary conditions used in the calibration. Four analyses for the Pure Flow condition and four for the Part Flow condition are considered.

The following observations can be made from Fig. 8:

- For both short and long penetrations ($z/D = 0.125$–1) and for both Pure Flow and Part Flow, the gradient around the tip is similar (same length between potential lines).
- For the Pure Flow penetration condition (Fig. 8), downward seepage flow occurs on the outside of the caisson, which leads to an increase in vertical effective stresses and an increase in penetration resistance.
- For the Part Flow condition with a short distance to an impermeable approaching layer ($z_b/D = 0.125$ in Fig. 8), the gradient is smaller than that for the Pure Flow condition, which leads to increased penetration resistance.

It can be seen that the mechanism controlling penetration resistance changes from case to case, and it is not possible to unambiguously conclude that the model will always over- or underestimate predictions. Even though the flow cases are different, a suction corresponding to a critical gradient is applied to both and it may therefore be assumed that the reduction model can be used as a reasonably good approximation. Further studies will be needed to confirm this assumption.

Time to Reach Steady State

Fully coupled analyses were performed assuming a steady-state flow condition to calibrate a model that can predict the critical

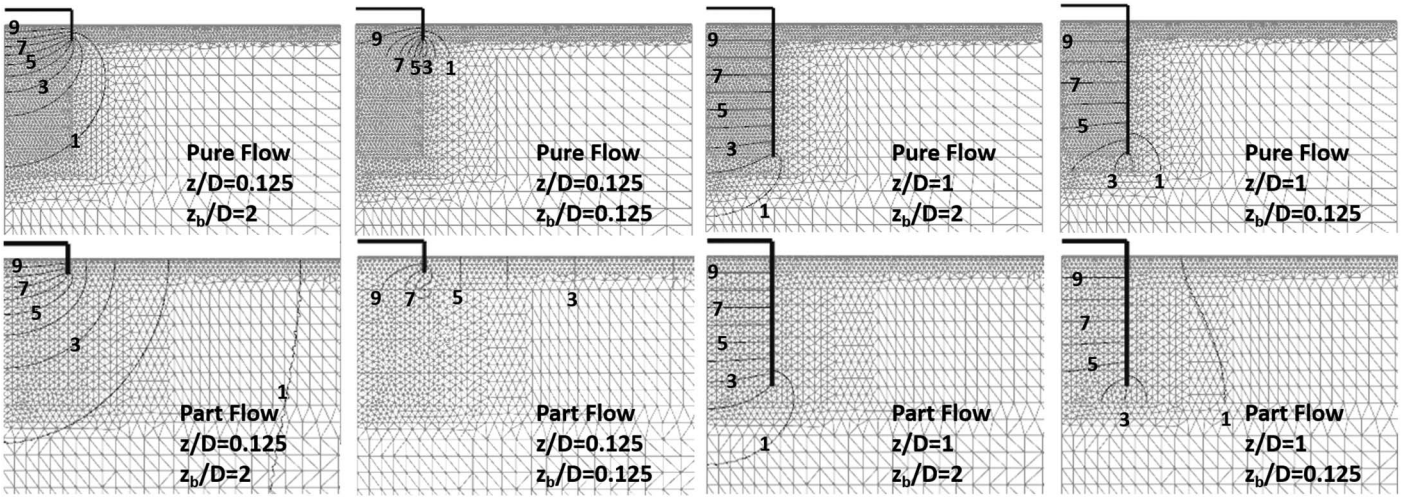

Fig. 8. Water head potential lines for different flow conditions.

Table 1. Approximate time to reach steady state from the FE analyses, assuming M = 67,310 kN/m^2, $k_o = 10^{-4}$ m/s, and $\gamma' = 10$ kN/m^3

		Pure flow		Part flow	
z/D	z_b/D	$k_i/k_o = 1$ (s)	$k_i/k_o = 5$ (s)	$k_i/k_o = 1$ (s)	$k_i/k_o = 5$ (s)
1	0.0125	207	163	1,973	1,476
1	2	287	196	2,326	1,558
0.125	0.0125	15	9	1,371	392
0.125	2	39	14	1,371	632

suction number. In reality, some time is required before a steady-state flow condition is achieved. Eight transient flow analyses were performed for the Pure Flow and Part Flow conditions in order to evaluate the time required to reach a steady state. Table 1 shows the approximate time until steady-state flow is reached. As may be expected, the time to reach steady state is much shorter for the Pure Flow case than for the Part Flow case because of the much shorter drainage path. It should be noted that these analyses are done by applying a pressure difference to a foundation under wished-in-place conditions at a given penetration depth. When a suction caisson is penetrating into the ground, a differential pressure has already been established in the previous installation depth. The actual time required to reach steady-state conditions at a new depth is approximated as the difference between the time it takes to reach steady state at the previous depth and the time to reach it at the new depth.

In order to analyze the FE results further, the time is normalized as proposed in Eq. (9) using the permeability inside the caisson, the oedometer stiffness of the soil (M), the effective unit weight (γ'), and a presumed representative drainage path of the water flow ($z + 2D$). Because it was impossible to find a unique drainage length given the different drainage conditions, the presumed drainage length was chosen based on trial and error

$$T = \frac{t \times k_i \times M}{\gamma'(z + 2D)^2} \tag{9}$$

Fig. 9 shows the results of the analyses shown in Fig. 8, now as normalized pressure head ($\Delta H/H$) versus normalized time. It is seen that the chosen normalization does not yield a unique relation

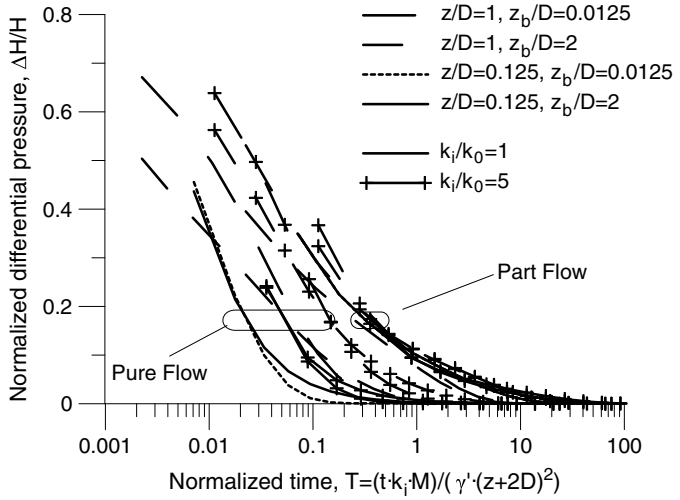

Fig. 9. Normalized pressure head versus normalized time, where H is applied pressure difference at T = zero.

for Pure Flow conditions, but appears to work reasonably well for Part Flow conditions. This is again related to the change in drainage path. The proposed normalization is used later to estimate the soil plug lift for the Part Flow condition.

From Fig. 9, it can be seen that, for Part Flow conditions, the pressure decreases continuously. At a normalized time, $T = 0.1$, it is about 30%; at $T = 1$, it is about 15%; and at $T = 10$, it has reached a steady state. Noticeably, the presence and distance of an underlying and gradually approaching impermeable layer seems to have no effect on the result. Although the analyses were performed with an elastic soil model that did not capture stress dependency, it is believed that the suggested approach provides a reasonable basis for assessing the time to reach-steady state conditions.

Plug Lift

One of the main assumptions of the Part Flow model is that seepage flow is developed in the permeable sand layer, which is overlain by an impermeable layer. This can be achieved either by developing cracks in the soil plug above this permeable sand layer or by lifting the complete soil plug within the skirt compartments and thereby triggering the seepage flow required to reduce stresses in the soil and hence penetration resistance. It may not be acceptable, however, that the plug lift/heave is so high that a gap forms below the sealing layer or that an excessive loosening of the sand layer occurs. Thus the plug lift/heave potential needs to be assessed and has to be limited to an acceptable value. To estimate the plug lift, a simple, yet reasonably accurate method that generates sufficient flow is proposed.

The plug lift is evaluated using the average flow required to generate sufficient flow, q, from Eq. (3) for the critical suction ($S_{N,\mathrm{cr}}$) value from Eq. (4) and the additional time it takes to reach steady state at the corresponding depth (Δt_{ss}). The heave is evaluated using the time to reach steady state multiplied by the corresponding steady-state flow. This is a simplification because the rate prior to steady state will be different from the steady-state flow rate. Both the time and the flow are functions of current penetration depth into the permeable layer (z). Based on Fig. 9, it is reasonable to expect that steady state is reached at a normalized time equal to $T = 1$. Using this time together with Eq. (9) enables calculation of the time required to generate steady-state conditions at the new depth. This is used together with the flow which is a function of the differential pressure required at the top of the permeable layer (Δu_{eq}).

To calculate the plug lift needed to generate sufficient flow, the following methodology is proposed:

1. Calculate the equivalent pressure Δu_{eq} as detailed in the calculation procedure for resistance reduction.
2. Calculate the equivalent water head as $H_{\mathrm{eq}} = \Delta u_{\mathrm{eq}}/\gamma_w$.
3. Use the equivalent water head result together with Eq. (3) to calculate the average flow needed, $q(z)$.
4. Calculate the time to reach steady state at that depth in each step as

Table 2. Soil profile for Examples 1 and 2

Example	Unit	Soil description	z_{pen} (m)	z_{pen}/D	γ' (kN/m^3)	q_c (kPa)	s_u^C (kPa)	ϕ' (degrees)
1	II	Very soft to firm clay	0.0–4.0	0.0–0.44	9	0–1	12–54	—
	III	Soft to stiff sandy clay	4.0–5.5	0.44–0.61	9	3–5	120–150	—
	III	Soft to stiff sandy clay	5.5–6.2	0.61–0.68	9	2	88	—
	IV	Loose to medium dense clayey sand	6.2–9.0	0.68–1.00	9	5–20	—	38
2	I	Silty clay	0.0–2.5	0.0–0.44	9	0–2	10	—
	II	Dense sand	2.5–7.0	0.44–0.61	10	19	—	44

$$t_{ss}(z_i) = \frac{\gamma'(z+2D)^2}{k_i \times M} \cdot T_{ss}$$

$$\Delta t_{ss}(z_i) = t_{ss}(z_i) - t_{ss}(z_{i-1})$$

5. Calculate the soil heave for each depth as

$$z_{heave}(z) = \sum \Delta t_{ss}(z) \times q(z)$$

Calculation of the plug lift is included in the general penetration algorithm; the required pressure difference together with the estimated plug lift is then an outcome of the analysis. The allowable plug lift and pressure difference needs to be evaluated from case to case. This calculation will overestimate the plug lift because it assumes that the skirt will penetrate only after reaching steady-state conditions. The penetration will most likely start before reaching steady-state conditions.

Loosening of Permeable Layer

When a skirt penetrates into a permeable layer with seepage flow, the soil inside the caisson will loosen. The combination of reduction in effective stress, seepage gradient and shearing, will loosen the permeable soil layer trapped within the caisson. This loosening of the soil plug is important to understand not only because it is related to change in the permeability ratio k_i/k_o, which is an input parameter to the model, but also because the state of the soil trapped inside the caisson after installation and some distance below the skirt will control the in-place performance of the caisson. For both Pure Flow and Part Flow conditions, the vertical effective stresses at the top of the permeable layer inside the caisson are zero. The geometry of the foundation will also be the same between the two cases, but the flow condition will be different. Even though the flow cases are different, a pressure difference corresponding to a critical gradient is applied in both cases; it is therefore assumed that the mechanism controlling the loosening of the soil plug is identical for the Pure Flow and the Part Flow cases. For this reason, it is recommended to calculate the loosening of the soil based on the geometry of the caisson and the dilatancy of the soil. This method is described in Andersen et al. 2008.

Demonstration of the Extended Model

To demonstrate the model, two analyses of suction anchor installations in layered soil profiles are back-calculated.

Example 1

Saue et al. (2017) presented the installation records for a suction anchor installed in a soil profile that is summarized in Table 2. The soil profile consists of two clay units (II and III) overlying a sand unit (IV). In Saue et al. (2017), the given strength profile was used together with a best estimate sensitivity factor of 2.2 in the clay layers (Units II and III) and strength anisotropy ratios of $s_u^{DSS}/s_u^C = 0.8$ and $s_u^{AV}/s_u^C = 0.6$. In the sand layer, an earth pressure coefficient of $K = 0.8$ was used together with a ratio between inside and outside permeabilities estimated to be $k_i/k_o = 5$ and with an effective friction angle derived from the measured tip resistance (q_c) of the CPT and the database of sands presented in Andersen and Schjetne (2013). An oedometer modulus of $M = 40{,}000$ kPa together with an outside permeability of $k_o = 10^{-5}$ m/s was used for the plug lift analysis. The following parameters were not presented in Saue et al. (2017) and, as a result, were estimated for this analysis: k_i/k_o, M, k_o, and t.

The diameter of the anchor was $D = 9$ m, with an assumed skirt wall thickness of $t = 0.06$ m and a skirt length of $s = 12.5$ m. During installation, cycling of the differential water pressure was started after 7 m of penetration to reduce the differential pressure between the inside and the outside of the skirt. Thus, only penetration resistance to a depth of 7 m prior to the onset of cycling is considered in the following. For more details see Saue et al. (2017).

Fig. 10 shows a comparison between the recorded measurements from installation, the predictions using the No Flow model, and the predictions using the extended Flow model. As expected, it can be seen in the clay layer that the extended Flow and the No Flow models are identical. However, when the skirt tip starts to penetrate into the sand layer, the two models start to deviate. The No Flow model assumes that the clay above the sand layer makes a seal that prevents any seepage flow around the skirt tip, whereas the extended Flow model assumes that the clay plug is lifted and generates seepage flow in the underlying sand layer. The responses of the two models are fundamentally different. The resistance increases markedly in the No Flow model and decreases in the extended flow model. The reason for the increase in resistance in

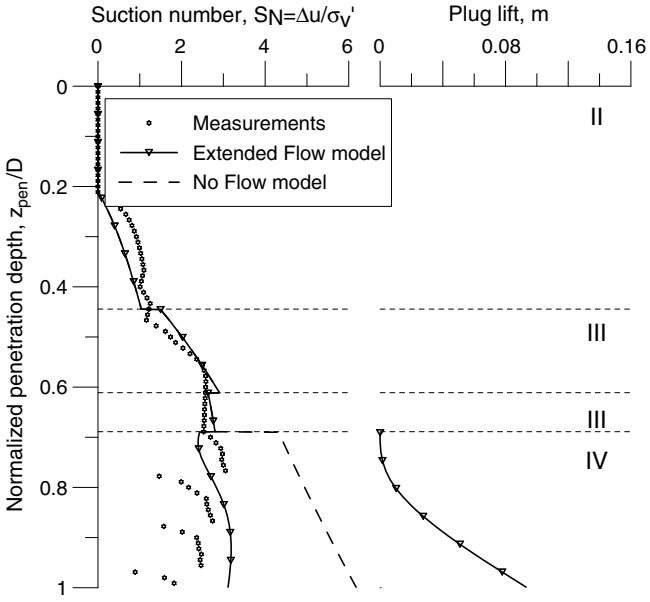

Fig. 10. Normalized pressure difference during installation for Example 1.

the No Flow model is that the sand has a very high tip resistance. The reason for a drop in resistance in the extended Flow model is that it assumes that the flow in the soil reduces stresses so much that tip resistance disappears. In this particular case, it can be seen that the equivalent weight of the anchor is $W'_{eq} = 0$ because the outside penetration resistance in the clay layers is greater than the weight of the anchor and the clay part of the soil plug. Resistance is therefore calculated to be zero when using Fig. 2 for initial penetration into the sand layer. When looking at the measurement data from the installation in Fig. 10, it is clear that the big increase in resistance predicted by the traditional Flow model does not match the observation. Even though the extended Flow model does not provide a perfect match, it seems to capture the observation better. In order to fit the observation, a relatively large ratio between inside and outside permeabilities was used. This change in permeability cannot be explained only by dilation in the sand but must also be related to the soil plug lift and seepage flow that may force additional change in the relative density of the sand layer.

The plug lift estimate in this example accumulates during penetration in the permeable layer. At a penetration depth of $z = D$, the plug lift is found to be relatively small and acceptable for a design case.

Example 2

Panayides et al. (2017) presented another case of a suction anchor installation in layered soils. The available information on soil conditions for the actual site was limited, but the authors presented a q_c profile and a back-analysis of nearby anchor installations, on which the layering and soil parameters used here are based. The parameters used in the model are shown in Table 2. The soil parameters for the clay are based on a back-analysis and therefore represent the remolded average strength. A sensitivity factor of 1 and strength anisotropy ratios of $s_u^{DSS}/s_u^C = 1$ and $s_u^E/s_u^C = 1$ are assumed. In the sand layer, an earth pressure coefficient of $K = 0.8$ was used together with $k_i/k_o = 3.5$ and with an effective friction angle derived from the measured tip resistance (q_c) of the CPT and the database of sands presented in Andersen and Schjetne (2013). An oedometer modulus of $M = 60{,}000$ kPa together with an outside permeability of $k_o = 10^{-4}$ m/s was used for the plug lift analysis. The diameter of the anchor was $D = 7$ m, with an assumed skirt wall thickness of $t = 0.04$ m and a skirt length of $s = 6.5$ m. The following parameters were not presented in Panayides et al. (2017) and were estimated for this analysis: k_i/k_o, M, k_o, and t.

Fig. 11 shows a comparison between recorded measurements from the installation, predictions using the No Flow model, and predictions using the extended Flow model. Similar observations as for Example 1 are seen in Example 2. In the clay layer, the extended Flow and No Flow models provide identical results. However, the moment the skirt tip starts to penetrate into the sand layer, the two models begin to deviate. The No Flow model assumes that the clay above the sand layer makes a seal that prevents any flow around the skirt tip, whereas the extended Flow model assumes that the clay plug is lifted and generates seepage flow in the underlying sand layer. Again, the responses from the two models are fundamentally different. The proposed extended Flow model accurately predicts the behavior observed in data measured during installation for the given k_i/k_o ratio, and again it can be seen that the plug lift is acceptable.

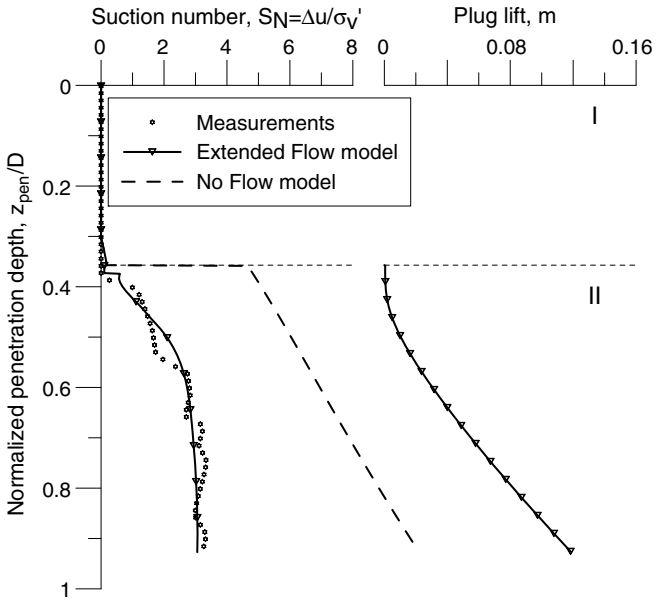

Fig. 11. Normalized pressure difference during installation for Example 2.

Design Considerations

The estimation of plug lift is based on the assumption that a pressure difference that is large enough to generate a critical gradient in the soil is applied. If an insufficient differential pressure is applied during installation, the critical gradient is not reached; if the differential pressure is kept constant, the soil plug is lifted without any further penetration. This is an unacceptable situation, and therefore it is important to have sufficient pumping capacity during installation so that the required pressure differential can be applied and adjusted in real time. Further, careful attention from the pump operator is needed to ensure that the differential pressure is high enough and that the caisson continuously penetrates.

Another possibility is that the plug does not lift but instead cracks develop and drainage occurs through the impermeable layer. The extended Flow model would still be applicable in this situation.

The evaluation of plug lift will be needed on a case-to-case basis and will depend on factors such as loads, geometry, and soil conditions. It must be ensured that plug heave and lift do not exceed what has been assumed in design, as insufficient skirt penetration would result if the plug were to reach the top lid. It is also noted that plug heave and lift have the potential for increased settlements after installation and thus be more severe for a bottom fixed structure than for an anchor application.

The model assumes that an infinite extent of the permeable layer is present. This is needed in order to make sure that there is sufficient water to generate the critical water flow gradient. When using the model, it is therefore important to make sure that the extent of the permeable layer is available or that the extent is sufficiently great for the permeable unit to hold enough water to produce a flow situation and the required gradients. This can be achieved by careful planning of geotechnical and geophysical site investigations. In case the extent of the permeable layer is unclear or known to be too limited for a flow situation to develop, the original model proposed by Andersen et al. (2008) or any other model developed for undrained penetration resistance can be used.

From back-analyses of field cases, it was observed that a relatively high estimate of inside permeability was needed in order to back-analyze the results. This indicates that the change in density in the Part Flow case is not only due to shearing but is also related to loosening from seepage flow. A higher value may therefore be used in design. It is recommended to evaluate the change in density from the plug lift estimate and use this change together with

change from shearing to estimate the ratio of the outside and inside permeabilities.

Conclusion

An extended flow model was presented that can be used for penetration analysis of skirted foundations installed with suction in layered soils. The proposed flow model is an extension of the model proposed by Andersen et al. (2008) that includes the effect of impermeable layers underneath and/or above a permeable layer. The model can be used together with traditional penetration models based on either bearing capacity or CPT. It is founded on an extensive finite-element parametric study, with its performance demonstrated on two large-scale installation cases where it was shown that it has the potential to more accurately predict actual required suction pressure than traditional models that assume no seepage flow in the sand layers covered by an impermeable layer. The model assumes that the impermeable part of the soil plug within the skirt is lifted and generates flow underneath.

A model was proposed to predict plug lift based on both time to reach steady-state conditions and flow required to generate a critical gradient. This model can be used to check if the target penetration depth can be reached with an acceptable plug lift value. It was shown that, for actual installation cases, this was achieved. Installation in layered soil profiles is critical, but if attention is given to pumps and operation, this extended flow model provides a tool to minimize uncertainties related to installation of skirted foundations in layered soil. This increases the application range of suction caissons, hence enabling an optimized foundation design.

Acknowledgments

This study was supported by base funding from the Research Council of Norway (NRF). The authors gratefully appreciate this support.

References

Aas, P. M., M. Saue, and J. Aarsness. 2009. "Design predictions and measurements during installation of suction anchors with and without water-flow system to help installation through layered soil profiles." In *Proc., Offshore Technology Conf.* Houston: Offshore Technology Conference.

Andersen, K. H., H. P. Jostad, and R. Dyvik. 2008. "Penetration resistance of offshore skirted foundations and anchors in dense sand." *J. Geotech. Geoenviron. Eng.* 134 (1): 106–116. https://doi.org/10.1061/(ASCE)1090-0241(2008)134:1(106).

Andersen, K. H., J. D. Murff, M. F. Randolph, E. C. Clukey, C. T. Erbrich, H. P. Jostad, B. Hansen, C. Aubeny, P. Sharma, and C. Supachawarotem. 2005. "Suction anchors for deepwater applications." In *Proc., Frontiers in Offshore Geotechnics (ISFOG) I*, 3–30. London: Taylor & Francis.

Andersen, K. H., and K. Schjetne. 2013. "Database of friction angles of sand and consolidation characteristics of sand, silt, and clay." *J. Geotech. Geoenviron. Eng.* 139 (7): 1140–1155. https://doi.org/10.1061/(ASCE)GT.1943-5606.0000839.

Erbrich, C. T., and T. I. Tjelta. 1999. "Installation of bucket foundations and suction caissons in sand: Geotechnical performance." In *Proc., Offshore Technology Conf.* Houston: Offshore Technology Conference.

Houlsby, G. T., and B. W. Byrne. 2005a. "Design procedures for installation of suction caissons in sand." *Proc. Inst. Civ. Eng. Geotech. Eng.* 158 (3): 135–144. https://doi.org/10.1680/geng.2005.158.3.135.

Houlsby, G. T., and B. W. Byrne. 2005b. "Design procedures for installation of suction caissons in clay and other materials." *Proc. Inst. Civ. Eng. Geotech. Eng.* 158 (2): 75–82. https://doi.org/10.1680/geng.2005.158.2.75.

Hvorslev, M. J. 1951. *Time lag and soil permeability in ground-water observations: Waterways experiment station, Bulletin No. 36*, 1–50. Vicksburg, MS: USACE.

Panayides, S., T. A. Powell, and K. Schrøder. 2017. Penetration resistance of suction caissons in layered soils: A case study. In *Proc., Offshore Site Investigation and Geotechnics, OSIG 2017*, 562–569. London: Society for Underwater Technology.

Saue, M., P. M. Aas, K. H. Andersen, and E. Solhjell. 2017. "Installation of suction anchors in layered soils." In *Proc., Offshore Site Investigation and Geotechnics, OSIG 2017*, 507–515. Houston: Offshore Technology Conference.

Senders, M., M. Randolph, and C. Gaudin. 2007. "Theory for the installation of suction caissons in sand overlaid by clay." In *Proc., 6th Offshore Site Investigation and Geotechnicics Conf.: Confronting New Challenges and Sharing Knowledge*, 429–438. Houston: Offshore Technology Conference.

Senders, M., and M. F. Randolph. 2009. "CPT-based method for the installation of suction caissons in sand." *J. Geotech. Geoenviron. Eng.* 135 (1): 14–25. https://doi.org/10.1061/(ASCE)1090-0241(2009)135:1(14).

Sturm, H. 2017. "Design aspects of suction caissons for offshore wind turbine foundations." In *Proc., 19th Int. Conf. on Soil Mechanics and Geotechnical Engineering TC209 Workshop (Foundation Design of Offshore Wind Structures)*. Seoul: Norwegian Geotechnical Institute.

Tjelta, T. I. 1994. "Geotechnical aspects of bucket foundation replacing piles for the Europipe 16/11 Jacket." In *Proc., Offshore Technology Conf.* Houston: Offshore Technology Conference.

Tjelta, T. I. 2015. "The suction foundation technology." In *Proc., Frontiers in Offshore Geotechnics (ISFOG) III*, 85–93. Houston: Offshore Technology Conference.

Tran, M. N. 2005. *Installation of suction caissons in dense sand and the influence of silt and cemented layers*. Sydney, Australia: Univ. of Sydney School of Civil Engineering.

Tran, M. N., and M. F. Randolph. 2008. "Variation of suction pressure during caisson installation in sand." *Géotechnique* 58 (1): 1–11. https://doi.org/10.1680/geot.2008.58.1.1.

Tran, M. N., M. F. Randolph, and D. W. Airey. 2005. "Study of seepage flow and sand plug loosening in installation of suction caissons in sand." In *Proc., 14th Int. Offshore and Polar Conf.*, 516–521. Houston: Offshore Technology Conference.

Tran, M. N., M. F. Randolph, and D. W. Airey. 2007. "Installation of suction caissons in sand with silt layers." *J. Geotech. Geoenviron. Eng.* 133 (10): 1183–1191. https://doi.org/10.1061/(ASCE)1090-0241(2007)133:10(1183).

Watson, P. G., C. Gaudin, M. Senders, and M. Randolph. 2006. "Installation of suction caissons in layered soil." In Vol. 1 of *Proc., Int. Conf. 6th, Physical Modelling in Geotechnics*, 685–692. London: Taylor & Francis.